2002

Water Transport in Polymer Electrolyte Membrane Electrolyzers Used to Recycle Anhydrous HCl: I. Characterization of Diffusion and Electro-osmotic Drag

Sathya Motupally
University of South Carolina - Columbia

Aaron J. Becker

John W. Weidner
University of South Carolina - Columbia, weidner@engr.sc.edu

Publication Info

Journal of the Electrochemical Society, 2002, pages D63-D71.

Publisher's link: http://dx.doi.org/10.1149/1.1464135
DOI: 10.1149/1.1464135

Journal of The Electrochemical Society, **149** (5) D63-D71 (2002)
0013-4651/2002/149(5)/D63/9/$7.00 © The Electrochemical Society, Inc.

Water Transport in Polymer Electrolyte Membrane Electrolyzers Used to Recycle Anhydrous HCl

I. Characterization of Diffusion and Electro-osmotic Drag

Sathya Motupally,[a,c,*,z] Aaron J. Becker,[b,*] and John W. Weidner[a,*]

[a]*Center for Electrochemical Engineering, Department of Chemical Engineering, University of South Carolina, Columbia, South Carolina 29208, USA*
[b]*E. I. DuPont de Nemours and Company, Central Research and Development, Wilmington, Delaware 19880-0323, USA*

In this paper, diffusion and electro-osmotic drag of water across Nafion® membranes in the presence of HCl are characterized. For all the measurements, one side of the Nafion membrane was in contact with liquid water and the other side with gaseous anhydrous HCl. To characterize diffusion of water, the open-circuit flux of water across a catalyst-coated Nafion 115 membrane was measured as a function of HCl flow rate and temperature at a constant cell pressure of 1 atm. Due to the nature of varying driving force for diffusion as a function of HCl flow rate, the experimental data was analyzed in conjunction with a mathematical model. The mathematical model accounts for condensation of water and is used to calculate the concentration of liquid hydrochloric acid in contact with the membrane. The mathematical model presented here is general and can be applied to the characterization of water transport across Nafion membranes in the presence of any gas that is soluble in water. In the case of HCl, at low inlet flow rates (<1500 cm^3/min, STP), the diffusion of water across the membrane is primarily governed by the diffusional limitations of HCl in the condensed phase. At high flow rates (>3000 cm^3/min, STP), the flux of water is a constant and depends on the saturation solubility of HCl in the condensed liquid phase. To measure the electro-osmotic drag parameter, the net flux of water across the membrane was measured as a function of the applied current density at high HCl flow rates (*i.e.*, uniform water flux). At 80°C, it was found that 3.8 mol of water per mole of protons are transported from the anode to the cathode.
 [DOI: 10.1149/1.1464135]

Manuscript submitted August 24, 2001; revised manuscript received November 6, 2001. Available electronically March 29, 2002.

In the chemical industry, chlorine is one of the most widely used feedstocks.[1] More than 50% of the chlorine used in the chemical industry ends up as hydrogen chloride, a waste byproduct.[2] For example, in the poly(vinylchloride) (PVC) and polyurethane industries, millions of tons of HCl gas are produced as a waste byproduct. Complete reclamation of the material value of chlorine used in such industries is only possible via recycling chlorine. Recycling chlorine can be accomplished by conventional thermochemical or by electrochemical processing.[2-10] Due to a negative reaction entropy change (ΔS), at all practical temperatures, only electrochemical processing affords direct conversion of HCl to chlorine and hydrogen. Electrochemical oxidation can either be liquid or gas phase.[2,6-10]

The gas-phase electrochemical conversion of HCl to chlorine and hydrogen was invented by DuPont in 1996.[6] The electrolysis is carried out in an electrolyzer similar to a H_2-O_2 polymer electrolyte membrane (PEM) fuel cell. The DuPont electrolyzer contains flow channels and gas diffusion backings on the anode and the cathode. The flow channels, the gas diffusion backings, and the membrane processes involved in the HCl electrolyzer are depicted in Fig. 1. In the figure, flow channels 1 and 2 represent the anode and the cathode, respectively. The anode and the cathode are separated by a catalyst-coated polymer electrolyte membrane like Nafion. The flow channels and the gas diffusion backings facilitate the distribution of the process fluids and also carry the electronic current out of the cell. The process fluid on the anode side is anhydrous HCl, which reacts at the surface of the anode catalyst layer to yield chlorine via the reaction

$$2HCl(g) = Cl_2(g) + 2H^+(aq) + 2e^- \quad [1]$$

The protons produced at the reaction site are transported to the cathode catalyst layer through the anode catalyst layer and the Nafion membrane. Here the protons are reduced to hydrogen. The cathodic and overall reactions can be written as

$$2H^+(aq) + 2e^- = H_2(g) \quad [2]$$

$$2HCl(g) = H_2(g) + Cl_2(g) \quad [3]$$

Nafion is a copolymer of a vinyl ester and tetrafluoroethylene and also contains conducting sulfonic acid side chains.[11-18] Nafion acts as the separator and the cation conducting electrolyte. Nafion is effective as a cation conductor only when sufficient water is associated with the sulfonic acid groups.[11-18] Therefore in an attempt to keep the membrane sufficiently hydrated, water is circulated through the cathode of the electrolyzer.

On open circuit, due to a gradient in the activity, water diffuses from the water to the HCl gas side (see Fig. 1). When HCl is oxidized in the electrolyzer, water is transported with the protons conducted from the anode to the cathode due to electro-osmotic drag. During the operation of the electrolyzer, the net flux of water transported into the anode gas stream is equal to the flux due to diffusion minus the flux due to the electro-osmotic drag.

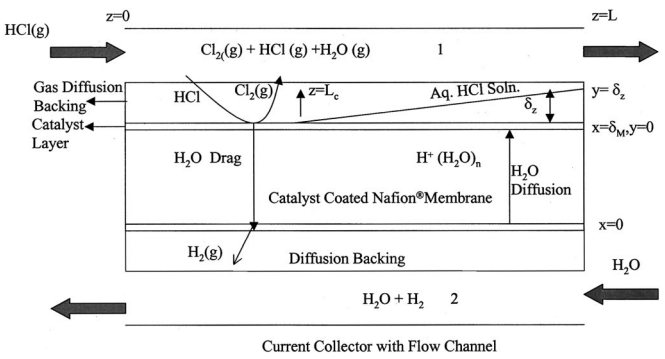

Figure 1. Schematic of the side view of the experimental cell. Dry HCl and water are fed to flow channels 1 and 2, respectively. Water diffuses across the Nafion membrane from the liquid to the gas side due to a gradient in the activity of water. After the condensation of water, the diffusion across the membrane is governed by the concentration of HCl in the condensed phase.

* Electrochemical Society Active Member.
[c] Present address: Duracell Global Science Center, Bethel, CT 06801.
[z] E-mail: sathya_motupally@gillette.com

The crossover of water across the membrane affects the quality of chlorine produced and also the electrochemical performance of the electrolyzer (due to the strong dependence of the Nafion properties on the water content). The water flux across the Nafion membrane in a HCl electrolyzer depends on the applied current density, temperature, and pressure of operation. From a process economics standpoint it is most desirable to operate the electrolyzer at the highest possible current density at the lowest possible voltage with a negligible net flux of water across the membrane. These conditions ensure the smallest footprint of the electrolyzer and the production of a dry chlorine stream. Therefore, process optimization requires the understanding of the diffusion and the electro-osmotic drag process across Nafion membranes.

The goal of this paper is to characterize the diffusion and the electro-osmotic drag across Nafion membranes in the presence of HCl. Previous water transport characterization across Nafion has been in the presence of fuel cell gases like H_2, O_2, and N_2.[13,15,17,18] There exist no reports in the literature regarding the transport of water across Nafion membranes when the more benign gases like hydrogen, oxygen, or nitrogen are substituted with an acidic gas like HCl. The main difference between the fuel cell gases and HCl is their solubility in water. In the case of HCl, water condensation readily results in the formation of hydrochloric acid and the solubility of the fuel cell gases in water is negligible. This feature leads to the main difference between the characterization of water diffusion in the presence of fuel cell gases and HCl. In the former case, the driving force for water diffusion is dictated by the activity of water in the vapor phase. In contrast, in the presence of HCl, the diffusion flux is governed by the vapor-phase water activity prior to condensation and the concentration of the hydrochloric acid in contact with the membrane after condensation (see Fig. 1).

In this work, we characterize water transport across catalyst-coated Nafion 115 membranes using a mathematical model in conjunction with experimental water flux data as a function of HCl flow rate, temperature, and applied current density. We apply the Fickian diffusion coefficient extracted from the water self-diffusion data reported in the literature[13] and the thermodynamic vapor-liquid equilibrium data to accurately predict the water flux as a function of the flow rate of HCl. Usng the temperature correction for the Fickian diffusion coefficient reported by Yeo and Eisenberg,[22] we also show that the temperature dependence of the water flux can be accurately predicted. Finally, using the net water flux data as a function of the applied current density at high HCl flow rates (*i.e.*, uniform water flux), we measured the electro-osmotic drag coefficient. The mathematical model presented in this work is general and can be used in conjunction with the appropriate input parameters and experimental data to characterize water transport across Nafion in the presence of any nonfuel cell gases.

Experimental

The water-flux measurements were carried out in a typical fuel cell setup. The fuel cell itself is comprised of Kynar®/graphite composite plates, stainless steel end plates, and copper current collectors. Water was fed to one side of the cell and the other side was fed with HCl gas. Both sides of the cell contained carbon cloth diffusion backings and flow channels machined into carbon paper. The flow channel was a single serpentine channel with a depth and width of 0.076 and 0.16 cm, respectively. The thickness of the diffusion backing was 600 μm with a porosity of approximately 65%. A Nafion 115 membrane with catalyst layers coated on both sides was sandwiched between the gas diffusion backings, and the cell was assembled by the application of a uniform torque of 35 in. lbs. between the copper plates on either side. The active area of the Nafion membrane was 50 cm^2. The catalyst layers contained 50/50 wt % of Nafion 1100 ionomer and catalyst. The thickness of the catalyst layer on each side was approximately 10 μm, and the active area of the membrane was 50 cm^2.

The temperature of the electrolyzer was controlled with the aid of heating cartridges and thermocouples on the anode and the cathode side. Water preheated to the cell temperature was circulated through one side of the electrolyzer and HCl passed through the other side. Water was delivered with the aid of a piston pump, and the pumping rate was always fixed so as to deliver 150 cm^3/min of water. HCl gas was fed to the cell without preheating. The flow rate of water and the temperature of the HCl gas at the inlet had negligible effect on the flux of water diffusing across the Nafion membrane.[18] The flow rate of HCl gas was controlled with the aid of a Brooks mass flow controller. The flow range of the controller was 30-4600 cm^3/min at STP. The pressure of each side of the cell was controlled with the aid of back pressure regulators, and the pressure was recorded with the aid of pressure gauges on the outlet and the inlet of either side of the membrane. All experiments were conducted under conditions where the pressure on both sides of the membrane was approximately the same.

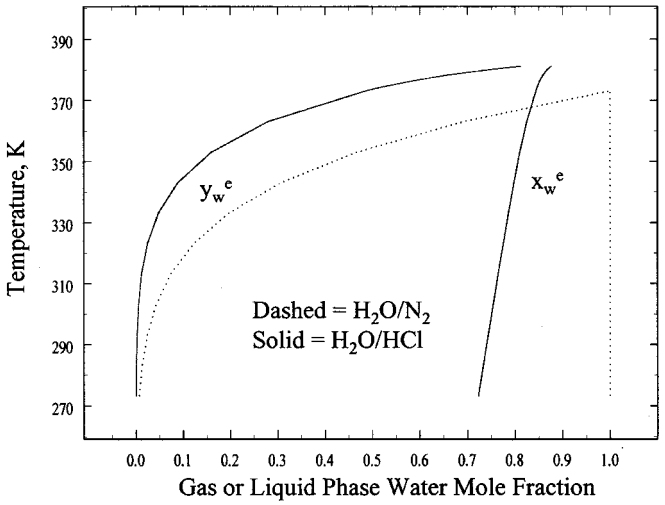

Figure 2. The *T-x-y* diagram (dew-point curves) for the nitrogen/water and HCl/water binary systems. In the presence of HCl, due to thermodynamic nondealities, water condenses at at lower water vapor mole fractions than in the nitrogen case.

The stream exiting the anode contained hydrochloric acid solution, water vapor, and HCl gas. This stream was passed through a vertical PVC knock-out vessel maintained at 20°C and at the cell pressure. Liquid hydrochloric acid and the water vapor in the exit stream condensed in the knock-out vessel. The vessel was equipped with a piezoelectric level sensor. The condensing liquid decreases the resonant frequency of the alternating signal emanating from the sensor, which was then correlated to a mass increase.[18]

The mass of the condensate was monitored continuously at 5 s intervals. The total flow rate of water leaving the anode side of the cell was calculated from the slope of the mass *vs.* time curves. As shown in our previous paper,[18] the mass *vs.* time data was linearly regressed to obtain the mass flow rate of hydrochloric acid condensing in the knock-out vessel. The resulting slope obtained from the linear regression of the mass *vs.* time data was multiplied by the equilibrium mole fraction of water (x_w^e) at 20°C (see Fig. 2). The data was collected at 60, 80, and 90°C and at a cell pressure of 1.0 atm. The resulting values correspond to the mass flow rate of pure water condensing in the knock-out vessel. Water is also associated with the vapor stream in equilibrium with the condensate in the knock-out vessel. The knock-out vessel is maintained at 20°C, and at this temperature the value of the vapor-phase mole fraction of water (y_w^e) is equal to 0.0023 (see Fig. 2). This means that at all the flow rates of HCl used in this work (0-4600 STP cm^3/min), more than 99% of the water leaving the electrolyzer is condensed in the knock-out vessel. Due to the negligible water vapor content, a correction was not applied and the mass flow rate of water exiting the electrolyzer was approximated to the water condensing in the

knock-out vessel. The total flux of water across the Nafion membrane is obtained when the mass flow rate of water is divided by the molecular weight of water (18 g/mol) and the area of the Nafion membrane (50 cm^2).

Model Development

In a previous paper,[18] we characterized water transport in Nafion 115 membranes as a function of water activity gradient across the membrane. In our work, one side was in contact with liquid water and the water activity gradient across the membrane was varied by varying the volumetric flow rate and pressure of nitrogen on the other side.[18] In this case, the driving force for water diffusion is a function of the position in the flow channel in the direction of flow. Therefore, the experimental water flux data was analyzed in conjunction with a mathematical model.

In the presence of HCl, the mathematical model we developed previously for the nitrogen case needs to be refined due to four unique reasons. First, the mole fraction of water at which condensation occurs is lower at all temperatures (see Fig. 2). The second unique feature of water crossover in the presence of HCl is related to water condensation. When water condenses, it forms concentrated hydrochloric acid in the gas-diffusion backing due to the high solubility of HCl in water. This results in a nonzero driving force for water diffusion across the membrane following condensation. The above-mentioned two features are represented in Fig. 2, which contains the dew-point curves for the water/HCl and water/N_2 binary systems. The dashed lines represent the water/N_2 system and the solid lines represent the water/HCl system. The gas-phase dotted line in Fig. 2 is the mole fraction of water at which condensation occurs at different temperatures and 1.0 atm in the presence of nitrogen. This line was generated by dividing the vapor pressure of water[15] by the total pressure of 1.0 atm. Since the solubility of nitrogen in liquid water is negligible, the resulting liquid phase is pure water (liquid phase is the dotted line in Fig. 2). The HCl data in Fig. 2 were generated by fitting an empirical expression to vapor/liquid equilibrium data obtained from OLI Systems Software at a pressure of 1.0 atm.[19] The resulting equilibrium relationships are (T is in kelvin)

$$y_w^e = 4.29 \times 10^{-12} \exp(0.068T) \quad [4]$$

$$x_w^e = -3.159 + 0.03928T - 1.22 \times 10^{-4}T^2 + 1.31 \times 10^{-7}T^3 \quad [5]$$

As seen from Fig. 2, the lower equilibrium gas-phase water mole-fraction in the HCl case means less water crossover is required before condensation occurs. Also, as mentioned earlier, upon condensation the activity of water unlike the nitrogen case is not unity and the diffusion flux is governed by the activity of water in the hydrochloric acid phase.

The third unique feature is a consequence of the condensation of hydrochloric acid. Continued diffusion of water in the presence of a condensed acid phase results in dilution. Only the liquid interface in contact with the HCl vapor is at the equilibrium concentration given by Eq. 5. The liquid interface in contact with the membrane is more dilute. The extent of dilution depends on the thickness of the condensed phase and the diffusion coefficient of HCl in water. Knowing the nonequilibrium concentration of water at the liquid/membrane interface is critical because it is this value that dictates the driving force for water diffusion across the membrane. Finally, HCl can be oxidized electrochemically according to Reaction 1. In the presence of an applied current, electro-osmotic drag decreases the rate of water transport across the membrane.

We build on the model developed in our previous paper,[18] which for this work is valid only until condensation occurs. As in our previous paper, we represent the serpentine flow configuration on the anode with a single parallel flow channel.[18] A three-dimensional end view of the anode flow channel is shown in Fig. 3. As seen in Fig. 3, the width, depth, and length of the channel are denoted w_1, d, and L, respectively. The width and thickness of the catalyst-coated Nafion membrane are denoted w_2 and δ_M, respectively. The assumptions used in the development of the model are

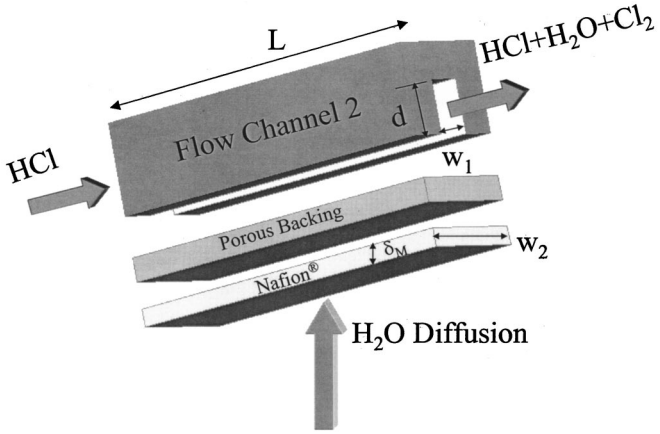

Figure 3. Schematic of a three-dimensional view of the single parallel channel representation. The width, depth, and length of the channel are denoted w_1, d, and L, respectively. The width of the catalyst-coated membranes is denoted w_2.

1. Prior to condensation, the Nafion membrane is the dominant resistance to the transport of water. Therefore, the concentration of water is uniform across the gas diffusion cloth and the flow channel.
2. The HCl/water vapor mixture in the flow channel obeys the ideal gas law.
3. After condensation, a solution of hydrochloric acid is formed at the membrane/gas diffusion-backing interface. The concentration of HCl at the condensate/gas interface is governed by equilibrium.
4. Diffusion of HCl across the membrane is negligible.
5. The thickness of the hydrated and the dry catalyst coated Nafion membranes are equal.
6. The entire fuel-cell system is maintained at a uniform and constant temperature throughout.
7. The permeability of water across the Nafion membrane is negligible.

Assumption 1 is valid because the diffusion coefficient of water vapor in HCl is at least four orders of magnitude greater than the diffusion coefficient of water in Nafion, while the diffusion lengths are comparable. The ideal gas law is valid at the pressures and temperatures employed here (*i.e.*, assumption 2). Assumption 3 is valid since the water enters the anode at the membrane/gas diffusion-backing interface. Upon condensation, HCl dissolves into the condensate and the hydrochloric acid solution is always in contact with the gas in the flow channel. Due to the fast kinetics of HCl dissolution, it is assumed that the condensate/gas mixtures are at equilibrium. Assumption 4 is based on experimental evidence. Pure water was fed to the cathode and its pH checked periodically. The flux of HCl across the membrane was measured by measuring the pH of the catholyte periodically. It was found that at all flow rates of HCl gas used in this work, less than 0.1% of HCl diffuses across the membrane into the catholyte. It has been shown that on equilibration with water, Nafion membranes swell. The thickness of hydrated Nafion membranes increases linearly with an increase in the water content.[15] For measurements on freely suspended Nafion membranes,[13] it is necessary to consider the variation in the thickness with the level of hydration. However, in our case, where the membrane is held tightly under pressure between graphite plates, it is assumed that the thickness of the membrane is invariant with the level of hydration (*i.e.*, assumption 5). The water flux data is taken at steady state, allowing the membrane surfaces to equilibrate (*i.e.*, assumption 6). A uniform and constant temperature (*i.e.*, assumption 6) was assured by placing a heating jacket around the carbon current collectors. The water flowing through one side of the cell was also

maintained at the same temperature as that of the cell. Although the HCl did not enter at this temperature, the data reported here was independent of the inlet temperature of the gas. Also, due to steady-state conditions, heating effects due to evaporation or condensation has no net effect on the cell's temperature. Finally, considering the fact that all experiments during this work were performed with approximately the same pressure on the water and gas sides, combined with the low permeability values of Nafion,[20] the permeability of water across the membrane is negligible (*i.e.*, assumption 7). In the following sections, the equations used to solve for the diffusion flux of water across the Nafion membrane are given.

Mass balances in the flow channel.—At the entrance of the anode flow channel (*i.e.*, $z = 0$, see Fig. 1 or 3), only gaseous HCl is present. However, due to the diffusion of water across the Nafion membrane, the mole fraction of water vapor in the flow channel increases in the z direction. Since it was determined experimentally that a negligible amount of HCl diffuses across the membrane, the molar flow rate of HCl does not vary in the z direction. This situation is identical to the case when nitrogen is the carrier gas.[18] The differential mole balance for water vapor in the flow channel can be represented mathematically as

$$\frac{N^{o}_{HCl}}{[1 - y_w(z)]^2}\frac{dy_w(z)}{dz} - \left(\frac{w_2}{w_1 d}\right)N_{w,x}(z) = 0 \qquad [6]$$

In the above equation, N^{o}_{HCl}, is the inlet molar flow rate of HCl and is related to its inlet volumetric flow rate, Q^{o}_{HCl}, by the following relationship

$$N^{o}_{HCl} = \frac{Q^{o}_{HCl}P}{RTA} \qquad [7]$$

For a complete listing of all the variables and symbols used in this work, the reader is referred to the List of Symbols section. In Eq. 6, $y_w(z)$ is the mole fraction of water in the vapor phase and $N_{w,x}(z)$ is the flux of water across the Nafion membrane. The driving force for $N_{w,x}(z)$ is given by the activity of water on the cathode side (*i.e.*, unity) and the activity of water in the vapor phase. [Note: the calculation of $N_{w,x}(z)$ is given in more detail separately in this section.] Assuming the ideal gas law, the activity of water in the vapor phase is given by

$$a_w = \frac{y_w P}{P^*(T)} \qquad [8]$$

In the above equation a_w is the activity of water on the anode, P the total pressure of the system, and $P^*(T)$, the saturated vapor pressure of water at the temperature of operation of the electrolyzer. Assuming that HCl/H_2O form an ideal gas mixture, the vapor pressure of water is described by the same expression that is used in the presence of gases like nitrogen[15]

$$\log[P^*(T)] = -2.18 + 0.029(T - 273.2) - 9.18 \times 10^{-5}(T - 273.2)^2 + 1.44 \times 10^{-7}(T - 273.2)^3 \qquad [9]$$

During the integration of Eq. 6, when the relative humidity of the HCl stream equals y^{e}_{w} (as given by Eq. 4), hydrochloric acid condenses. The value of z at which condensation starts is denoted L_c in Fig. 1. For all z greater than L_c, Eq. 6 does not apply. The water diffusing across the membrane is now distributed between the liquid and the vapor phases. In accordance with assumption 4, phase rule dictates that vapor-liquid equilibrium governs the concentration of HCl in the vapor phase and the surface of the condensate. Upon condensation, the water flux across the membrane can be calculated either by using a water or HCl balance in the flow channel. For this work, we use the HCl mass balance in the vapor and liquid phases in the flow channel.

After condensation, the total flow rate of HCl is still a constant, but now it is distributed between the two phases according to the following relationship

$$N^{o}_{HCl} = N^{v}_{HCl}(z) + \left(\frac{w_2\delta_z}{w_1 d}\right)N^{L}_{HCl}(z) \qquad [10]$$

Equation states that the HCl in the vapor phase is given by the difference between the total amount of HCl fed to the anode and the HCl that is dissolved in the liquid phase forming hydrochloric acid. In Eq. 10, N^{v}_{HCl} and N^{L}_{HCl} are the HCl molar fluxes in the vapor and liquid phases, respectively. Also, δ_z is the thickness of the condensed phase and is denoted in Fig. 1. The calculation of δ_z is based on the total volumetric flow rate of the condensed phase and the superficial velocity of the condensed phase through the gas diffusion backing. At the exit of the flow channel, the thickness of the condensed phase is related to the volumetric flow rate of the condensed phase through the equation

$$\delta^{o} = \left[\frac{Q^{L}(z = L)}{w_2 V^{L}}\right] \qquad [11]$$

In Eq. 11, Q^{L} is the volumetric flow rate of the condensed hydrochloric acid and V^{L} is the superficial velocity of the condensed phase. The volumetric flow rate of the condensed phase increases in the z direction and the superficial velocity remains a constant. Under the assumption that the thickness of the condensed phase increases linearly in the direction of flow, the volumetric flow rate can be related to the thickness of the condensed phase at the exit of the electrolyzer according to the equation

$$\delta_z = \delta^{o}\left(\frac{z - L_c}{L - L_c}\right) \qquad [12]$$

In Eq. 10, the liquid-phase molar flux of HCl can be related to the velocity and the average concentration of HCl, $\langle C_{HCl}\rangle$, in the condensed phase through the following equation

$$N^{L}_{HCl}(z) = V^{L}\langle C_{HCl}(z)\rangle \qquad [13]$$

In Eq. 11-13, information regarding the superficial velocity of the condensed phase is required. The condensed phase flows through the porous gas-diffusion backing on the anode due to a pressure drop across the flow channel (see Fig. 1). Therefore, the superficial velocity of the liquid phase in this porous region can be calculated using Darcy's law.[24] According to Darcy's law, the superficial velocity of a fluid in porous media is proportional to the pressure and gravitational forces acting on the fluid as follows

$$V^{L} = \left(\frac{\Delta P}{L} + \rho_{HCl}g\right)\frac{K}{\mu_{HCl}} \qquad [14]$$

Equation 13 also needs the calculation of $\langle C_{HCl}\rangle$.

At $z = L_c$, the water content of the condensate is given by Eq. 5. However, due to diffusional limitations for HCl in the condensed phase, water crossing the membrane dilutes the acid at the solution/membrane interface. Therefore, to calculate $\langle C_{HCl}\rangle$, a differential mole balance in the condensed phase is solved

$$V^{L}\frac{\partial C_{HCl}}{\partial z} = D_{HCl}\frac{\partial^2 C_{HCl}}{\partial y^2} \qquad [15a]$$

where V^{L} is the superficial velocity of the condensed liquid phase in the gas-diffusion backing and D_{HCl} is the diffusion coefficient of HCl in water. The boundary conditions for Eq. 15a can be written as

$$\text{at} \quad z = L - L_c, \; C_{HCl} = 0 \qquad [15b]$$

$$\text{at} \quad y = \delta_z, \; C_{HCl} = C^e_{HCl} \qquad [15c]$$

$$\text{at} \quad y = 0, \; \frac{\partial C_{HCl}}{\partial y} = 0 \qquad [15d]$$

Equation 15b states that the concentration of HCl at the condensation point is zero and Eq. 15d states that the flux of HCl across the Nafion membrane is zero. Equation 15c is the equilibrium relationship (see Eq. 5). An analytical solution to Eq. 15a-d is feasible, and the solution which is a function of y and z, can be represented as

$$C_{HCl} = C^e_{HCl} - \frac{4C^e_{HCl}}{\pi}\sum_{n=0}^{\infty}\frac{(-1)^n}{2n+1}\cos\frac{(2n+1)\pi y}{2\delta_z} \times \exp\left(-\left[\frac{(2n+1)\pi}{2\delta_z}\right]^2 D_{HCl}V^L z\right) \qquad [16]$$

To get the average concentration of HCl in the condensed phase for substitution into Eq. 13, Eq. 16 is integrated from y equal zero to δ_z to give

$$\langle C_{HCl}\rangle = C^e_{HCl}\delta_z - \frac{8C^e_{HCl}\delta_z}{\pi^2}\sum_{n=0}^{\infty}\frac{(-1)^n}{(2n+1)^2} \times \left(\cos\frac{(2n+1)\pi}{2\delta_z} - 1\right) \times \exp\left(-\left[\frac{(2n+1)\pi\pi}{2\delta_z}\right]^2 D_{HCl}V^L z\right) \qquad [17]$$

An expression for the surface concentration can be obtained from Eq. 16 by substituting $y = 0$ (*i.e.*, $x = \delta_M$). The resulting expression for the surface concentration can be written as

$$C^s_{HCl} = C^{eq}_{HCl} - \frac{4C^{eq}_{HCl}}{\pi}\sum_{n=0}^{\infty}\frac{(-1)^n}{2n+1} \times \exp\left(-\left[\frac{(2n+1)\pi}{2\delta_z}\right]^2 D_{HCl}V^L z\right) \qquad [18]$$

Material balance for liquid water across the membrane.—At steady state, the flux of water across the membrane, in the z direction, is a constant and given by

$$N_{w,x}(z) = -\frac{\rho_M}{M_M\delta_M}\int_{\lambda_c}^{\lambda_a} D_{w,F}\, d\lambda + \frac{\xi i}{F} \qquad [19]$$

The first term on the right side is the diffusional flux, which was derived previously.[18] The second term is the flux due to electro-osmotic drag.[15] In Eq. 19, the lower and upper limits of integration are the water content of the membrane at the cathode and anode interfaces, respectively. Zawodzinski *et al.*[12] measured the water content of Nafion membranes in contact with pure water, λ^o, to be 22 and 18 at 30 and 80°C, respectively. We assume here that λ^o varies linearly between these two temperatures to give the following relationship

$$\lambda^o = 53.3 - 0.10T \qquad [20]$$

Since the cathode is in contact with pure water, $\lambda_c = \lambda^o$.

Prior to condensation, the following equation for the water content of the membrane on the anode side, λ_a, is valid[14]

$$\lambda = 0.043 + 17.81a_w - 39.85a_w^2 + 36.0a_w^3 \qquad [21]$$

In Eq. 21, a_w is given by Eq. 8. After condensation, the water content of the membrane depends on the concentration of HCl in contact with the membrane. Balko *et al.*[21] measured the water content of Nafion 117 membranes as a function of the concentration of hydrochloric acid at 25°C. Their λ *vs.* C_{HCl} data is linear. Assuming that the slope of this linear relationship is independent of temperature, the following expression is obtained

$$\lambda_a = \lambda^o - 1200C^s_{HCl} \qquad [22]$$

The Fickian diffusion coefficient of water, $D_{w,F}$, also depends on the water content of the membrane.[13,18] As discussed previously,[18] the Fickian diffusion coefficient is related to the self-diffusion coefficient through the equation

$$D_{w,F}(\lambda) = D_{w,I}\underbrace{\left[\frac{\partial \ln(a_w)}{\partial \ln(\lambda)}\right]}_{\text{Darken factor}} \qquad [23]$$

Using the diffusion-coefficient data measured by Zawodzinski *et al.*[12] and the enthalpy of diffusion measured by Yeo and Eisenberg,[22] the following expression for the self-diffusion coefficient of water in Nafion 117 was obtained[18]

$$D_{w,I} = 1.9 \times 10^{-3}(\lambda - 0.0209\lambda^2 - 0.501)\exp\left[\frac{-2436}{T}\right] \qquad [24]$$

To evaluate the Darken factor in Eq. 12, information regarding the activity of water as a function of HCl concentration in liquid solutions is needed. Using OLI Thermodynamics Software,[19] we generated the following expression for the activity of water as a function of HCl concentration

$$a_w = 1 - 60C_{HCl} \qquad [25]$$

According to Eq. 25, the activity of water decreases from unity to 0.4 as the concentration of HCl in the acid solution increases from zero to 10^{-2} mol/cm^3. Equation 22 and 25 are combined, and the resulting equation is differentiated to get the Darken factor. Substitution of the Darken factor and Eq. 25 into Eq. 24 yields the following expression for the Fickian diffusion coefficient of water

$$D_{w,F} = \frac{2.5 \times 10^{-3}\lambda(\lambda - 0.0209\lambda^2 - 0.501)}{\lambda - 2}\exp\left[\frac{-2436}{T}\right] \qquad [26]$$

Solution procedure.—Prior to condensation, using Eq. 7-9 in conjunction with Eq. 6, the differential equation is solved for the single unknown, $y_w(z)$. During the integration, at every z, the $y_w(z)$ is compared to the y^e_w calculated by using Eq. 4. If $y_w(z)$ does not equal y^e_w then the total water flux of water leaving the flow channel at the exit is calculated using the equation

$$N_w = N^o_{HCl}\left(\frac{y_w(z=L)}{1 - y_w(z=L)}\right) \qquad [27]$$

After the condensation of water, the total water crossing the membrane is distributed in the vapor and the liquid phases. Assuming a value for Q^L at $z = L$, Eq. 10 is solved for in conjunction with Eq. 11-27. The solution procedure is iterative, and when the flux of water across the membrane equals the sum of the fluxes of water in the vapor and liquid phases, the iteration is stopped. That is, the solution is reached when at the exit of the flow channel the following equation is satisfied

$$w_1 d\frac{N^v_{HCl}}{1 - y^e_w} + w_2\delta_z N^L_{HCl}x^e_w - w_2\int_0^L N_{w,x}dz = 0 \qquad [28]$$

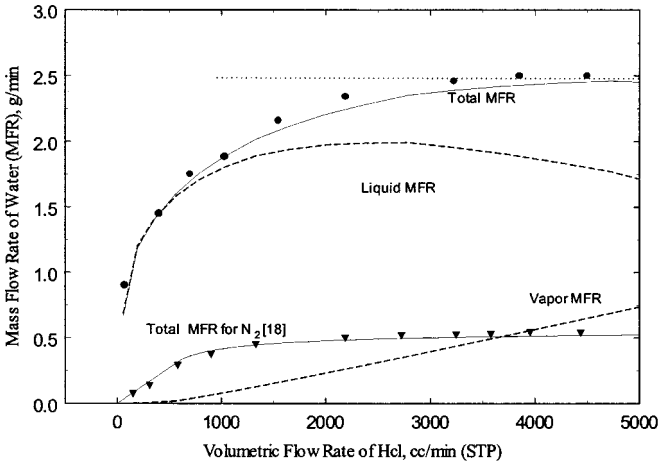

Figure 4. Experimental and model simulated mass flow rate (MFR) of water across the membrane from the cathode to the anode. The symbols represent experimental data and the solid curve represents model simulations using Eq. 6-28. The dashed lines represent the vapor and liquid phase contributions to the overall mass flow rate. The dotted line represents the predicted water mass flow rate assuming negligible HCl diffusional limitations in the condensed phase. The nitrogen data and the model simulations are reproduced from our previous paper.[18]

Table I. Parameters used in the simulations.

		Reference
Channel width (w_1)	0.15 cm	[a]
Channel depth (d)	0.076 cm	[a]
Diffusion coefficient of water ($D_{w,F}$)	Eq. 27	
Density of membrane (ρ_M)	2.0 gm/cm^3	15
Density of hydrochloric acid (ρ_{HCl})	1.1 gm/cm^3	22[b]
Length of channel (L)	136 cm	[a]
Length of gas diffusion backing (L_{GDB})	6.0 cm	[a]
Membrane width (w_2)	0.36 cm	[a,c]
Molecular weight of membrane (M_M)	1100 g/mol	15
Permeability of gas diffusion backing (K)	3.6×10^{-9} cm^2	[a]
Thickness of membrane (δ_M)	0.155 cm	[a]
Total pressure (P)	1.0 atm	[a]
Pressure drop (ΔP)	4.17×10^{-5} atm/STP cm^3	[a]
Vapor pressure of water (P^*)	Eq. 9	15
Water content (λ)	Eq. 22	21
Equilibrium vapor and liquid Mole fractions (y_w^e, x_w^e)	Eq. 4 and 5	19
Viscosity of HCl solution (μ_{HCl})	0.05 cp	19, 23[b]

[a] Indicates measured.
[b] Value corresponds to 5 M HCl solution.
[c] Area of membrane used = $w_2 \times L = 50$ cm^2. w_2 is calculated by dividing the membrane area with the effective length of the serpentine flow channel.

Results and Discussion

Experimental and model-simulated mass flow rate of water exiting the electrolyzer at 80°C and 1.0 atm cell pressure as a function of HCl volumetric flow rate are shown in Fig. 4. In Fig. 4, the curves represent model simulations and the symbols represent experimental data. The HCl model simulations were generated by considering diffusion limitations in the condensed phase (*i.e.*, by using Eq. 6-28). The list of parameters used in the simulations is given in Table I. The thermodynamic data required for the mathematical model were generated using the OLI Thermodynamic Systems Software.[19]

As seen in Fig. 4, the water flux across the membrane increases with an increase in HCl flow rate and gradually transitions to an asymptote at higher flow rates. For example, the mass flow rate of water increases from 0.6 to 1.9 g/min as the inlet volumetric flow rate of HCl increases from 75 to 1500 cm^3/min. With the increase in the flow rate beyond 1500 cm^3/min, the mass flow rate increases gradually and asymptotes at 2.5 g/min. For all HCl inlet flow rates greater than 3000 cm^3/min, the mass flow rate of water measured experimentally is a constant and equal to 2.5 g/min. As seen from Fig. 4, there is excellent agreement between the model simulations and the experimental data.

In Fig. 4, the water flux data across Nafion when nitrogen instead of HCl is used as a carrier gas are also shown. The nitrogen data is the same as presented in our previous paper and is used here to highlight the differences in the flux of water across the Nafion membrane with gas type.[18] As seen from the figure, there are two main differences between the HCl and nitrogen data presented. First, at the same volumetric flow rate of gas, the mass flow rate of water in the HCl case is approximately a factor of five greater than the corresponding nitrogen value. For example, at a flow rate of 4600 cm^3/min, the value of the mass flow rates with nitrogen and HCl cases are 0.5 and 2.5 g/min, respectively. This difference is the water crossover rates is due to the higher rate of diffusion when HCl is the carrier gas *vs.* nitrogen. The higher diffusion rate is due to the value of the Fickian diffusion coefficient of water in the membrane being approximately greater by a factor of five when equilibrated with hydrochloric acid solution *vs.* pure water. Note that the intrinsic diffusion coefficients of water in both the cases are assumed to be identical and given by Eq. 24.[13] However, the Fickian diffusion coefficients in the two cases are different due to the difference in the Darken factor given by Eq. 23. The Darken factor in the case of HCl includes the solution nonidealities and in the case of nitrogen, due to the negligible solubility of the gas in the solution, the Darken factor is derived assuming only vapor-phase equilibrium with the membrane. The Fickian diffusion coefficient for the nitrogen case is presented in Ref. 18.

The second difference between the nitrogen and the HCl data is related to the qualitative trends in the increase of water flux across the membrane in the presence of HCl and nitrogen are different. For example, the flux of water increases linearly with the volumetric flow rate of nitrogen and plateaus to a constant value at higher values of the volumetric flow rate. In the case of HCl, the flux of water also increases with an increase in the volumetric flow rate of HCl. However, the increase is not linear. The flux of water in the HCl case also plateaus to a constant value. This difference in the trends is due to the nature of the driving force for diffusion. In the case of nitrogen, the linear region is a result of water condensation. Upon condensation, the driving force for water diffusion is zero, and the water vapor mole fraction in the nitrogen stream is a constant and equal to y_w^e. The molar flow rate of water exiting the cell is therefore equal to the inlet molar flow rate of nitrogen multiplied by the constant value of $(y_w^e/1 - y_w^e)$ thereby leading to a linear behavior. In the case of HCl, due to the solubility of HCl in the liquid phase and continued diffusion upon condensation results in variable liquid and the vapor mole fractions of water and HCl as a function of the volumetric flow rate of HCl. Therefore, unlike the nitrogen case, a linear relationship between the flow rate and flux is not obtained. At high flow rates, the behavior in the case of nitrogen and HCl are identical and the water crossover rate is invariable with increasing volumetric flow rate of gas. The only difference between the two cases is the value of the maximum flux of water.

In Fig. 4, the vapor and liquid-phase water mass flow rates are also presented as a function of the volumetric flow rate of HCl (see dashed lines). At the exit of the electrolyzer, the sum of the mass flow rate of water in the liquid and the vapor phases is equal the

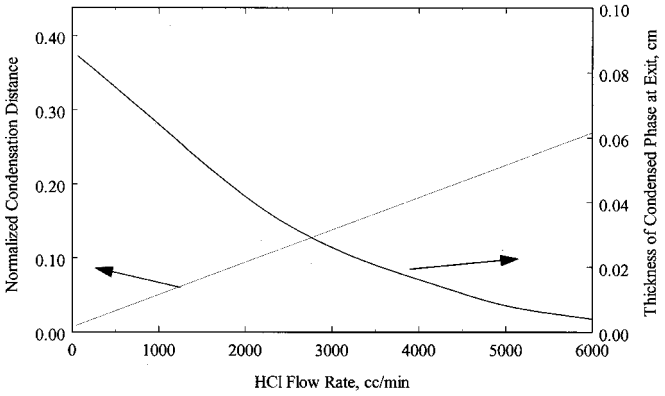

Figure 5. Normalized condensation length (L_c/L) and the thickness of the condensed phase as a function of HCl flow rate. The condensation length increases with an increase in the flow rate of HCl. This is due to the increase in the HCl mole fraction and therefore a relatively longer distance prior to the water vapor mole fraction equaling x_w^e. The thickness of the condensate decreases with an increase in the HCl flow rate due to a concomitant increase in the pressure drop across the cell.

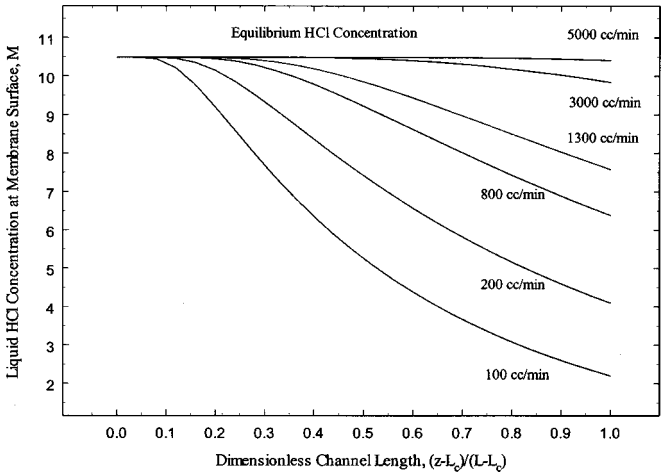

Figure 6. Simulated hydrochloric acid profiles at the surface of the Nafion membrane. With an increase in the volumetric flow rate of HCl, the resistance to the diffusion of HCl in the condensed phase decreases, and the concentration equals the equilibrium value through out the the thickness of the condensed phase. For flow rates greater than 3000 cm^3 /min, the average concentration is approximately equal to 10.5 M, the equilibrium value.

total mass flow rate of water. As seen from the figure, at low flow rates, the majority of the water diffusing across the membrane is contained in the liquid phase. For example at 500 cm^3/min flow rate, the liquid-phase mass flow rate is 1.6 g/min and accounts for more than 99% of the total water flux. With an increase in the HCl volumetric flow rate, the amount of water contained in the vapor phase increases. This increase is due to a relative reduction in the condensation effects. At all the flow rates, the mole fraction of water in the vapor phase is equal to y_w^e. At approximately 8000 cm^3/s of HCl flow rate (not seen in Fig. 6), the vapor- and liquid-phase fluxes are equal.

Water condensation effects are severe at lower flow rates. At all flow rates used in this work, water does condense due to the relatively lower value of y_w^e compared to the nitrogen case (see Fig. 2). The length of the flow channel that HCl gas traverses prior to condensation, L_c, as a function of gas flow rate is shown in Fig. 5. As seen in the figure, L_c, increases with an increase in the flow rate of HCl. This is due to a decrease in the mole fraction of water vapor in the flow channel resulting from increased gas mole fraction. At HCl flow rates less than 3000 cm^3/min, water condenses within 10% of the length of the channel. Even at the highest flow rate of HCl shown in Fig. 4 (6000 cm^3/min), water condenses to form hydrochloric acid within 25% of the channel length. As a means of comparison, when nitrogen is the carrier gas at 1.0 atm and 80°C, water does not condense at flow rates greater than 800 cm^3/min.[18]

As discussed above, due to the severe condensation problems at all flow rates used in this work, the majority of the diffusion flux is governed by the activity of water in the liquid phase. The activity of water is a function of the HCl concentration and therefore the nature of increase in the mass flow rate of water with HCl flow rate is controlled by the concentration of hydrochloric acid in the condensate. Once water condenses in the gas diffusion backing on the anode, it forms hydrochloric acid whose concentration is governed by vapor-liquid equilibrium and equal to the corresponding value of $1 - x_w^e$ at the operating temperature and pressure of the electrolyzer. For example, in the case of the 1.0 atm and 80°C operation, this concentration would translate to 10.5 M. In the absence of diffusional limitations (*e.g.*, very thin condensate layer in the backing), the concentration of the condensate layer would be equal to 10.5 M throughout the thickness. Under such conditions, the model predicts that the water crossover across the membrane would be a constant with volumetric flow rate of HCl and equal to 2.5 g/min. This is illustrated by the dotted line in Fig. 4.

However, in reality at all flow rates, the concentration only at the edge of the condensate layer (*i.e.*, at $y = \delta_z$ in Fig. 1) is dictated by the phase rule and is proportional to $1 - x_w^e$. The concentration at the surface of the membrane (*i.e.*, $y = 0$) depends on the HCl diffusional limitations. The HCl diffusional limitations in the condensate layer are directly proportional to the thickness of the condensate layer. After the onset of condensation, water diffusing into the anode is distributed in the liquid and vapor phases to maintain equilibrium and the HCl in the vapor phase does the same. As more water enters the anode, the thickness of the water condensate increases and the mole fraction of HCl throughout the thickness of the condensate is no longer equal to $1 - x_w^e$. A gradient in HCl concentration is encountered and the mole fraction of HCl in the condensed phase at the surface of the membrane (*i.e.*, at $y = 0$) is less than $1 - x_w^e$.

For any flow channel in a fuel cell or an electrolyzer, a pressure drop is required to enable flow. For the HCl electrolyzer, at 80°C and 1.0 atm operating pressure, the pressure drop between the entrance and the exit of the gas channel increases linearly from 0.01 to 0.2 atm with an increase in the flow rate from 50 to 4600 cm^3/min (STP). Darcy's law (Eq. 14) dictates that an increase in the pressure drop results in an increase in the superficial velocity of the condensate through the diffusion backing. This in turn results in the reduction of the thickness of the condensed phase. The thickness of the condensed layer at the exit of the electrolyzer as a function of HCl flow rate is shown in Fig. 5. As seen in the figure, with an increase in the volumetric flow rate from 250 to 3000 cm^3/min, the thickness of the condensed phase decreases from 800 to 200 μm. The reduction in the thickness of the condensed layer results in a decrease in HCl diffusional limitations.

A reduction in the diffusional limitations results in an increase in the average concentration of HCl at all zs. This is illustrated in Fig. 6. In this figure, the concentration of HCl at the surface of the anode membrane interface is plotted as a function of normalized z for five different inlet HCl flow rates. At all flow rates, the concentration of HCl in the condensed phase at $z = L_c$ is equal to the equilibrium value (10.5 M). This is a result of a zero thickness of the condensed phase at $[z - L_c/L - L_c] = 0$. As the condensed phase travels through the gas-diffusion backing, its thickness increases due to more water diffusing across the membrane. This results in an increase in the diffusional resistance for HCl. Therefore, the concentration of HCl at the surface of the membrane decreases with an

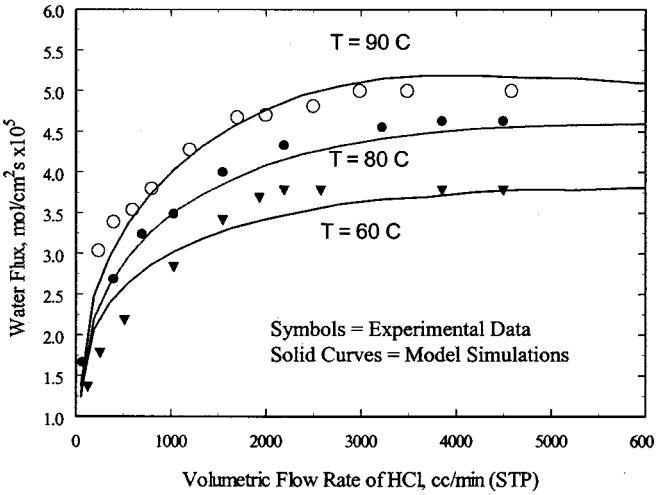

Figure 7. Experimental and model simulated water flux data as a function of volumetric flow rate of HCl and temperature. With an increase in temperature, the diffusion coefficient of water through Nafion increases and the equilibrium solubility of HCl decreases. However, the resultant is an increase in the flux of water.

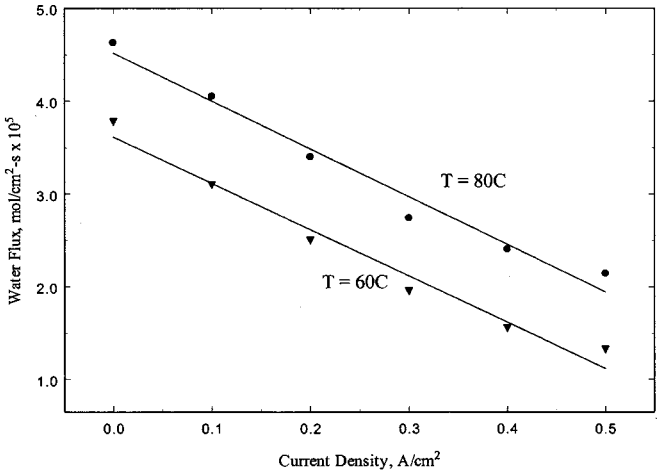

Figure 8. Resultant water flux due to diffusion and electro-osmotic drag as a function of current density. The experiment was performed at a flow rate of 5000 cm^3/min where the diffusion flux was found to be invariant with the flow rate of HCl. The slope of the straight lines are proportional to the electro-osmotic drag coefficient and equal to 3.8 mol of H_2O/mole of H^+.

increase in z. Also, at any z, the concentration of HCl at the surface of the membrane is greater at higher flow rates. For example at $z - L_c/L - L_c = 0.5$, the corresponding surface concentrations at HCl flow rates of 400, 900, 1200, 1700, and 5000 cm^3/min are 4, 7.8, 9.0, 10.5, and 10.5 M, respectively. This increase in the water flux is related to the decrease in the diffusional resistance with flow rate. As mentioned earlier, with an increase in the flow rate, the thickness of the condensed layer decreases due to an increase in the superficial velocity. This results in an increase in the average HCl concentration at the surface of the membrane. With an increase in the HCl surface concentration, the water content of the membrane on the gas side decreases (see Eq. 21) thereby resulting in an increased diffusional driving force. The maximum water crossover corresponding to a mass flow rate of 2.5 g/min is obtained when the surface concentration is 10.5 M at all zs. This is applicable to all HCl flow rates greater than 2500 cm^3/min. For all flow rates less than 2500 cm^3/min, the water crossover depends on the average concentration of HCl at the surface of the membrane.

A plot of experimental water flux data and model simulations as a function of HCl flow rate and cell temperatures of 60, 80, and 90°C are shown in Fig. 7. Note that the water flux across the membrane can be converted to a mass flow rate upon multiplication by 18 g/mol × 60 s/min × 50 cm^2. As seen in the figure, the flux of water increases with an increase in the flow rate of HCl and temperature. The model simulations match experimental data with less than 5% error at 80 and 90°C and 6% error at 60°C. Temperature affects not only the diffusion coefficient of water in Nafion but also the value of the equilibrium concentration of HCl. An increase in the cell temperature results in an increase in the diffusion coefficient of water and a decrease in the equilibrium concentration of HCl (see Fig. 2 or Eq. 6). An increase in the diffusion coefficient results in an increase in the diffusion flux. A decrease in the concentration of HCl in the condensed phase decreases the gradient in the water content across the membrane and therefore the driving force for diffusion. Therefore increasing the cell temperature results in two counteracting effects on the diffusion of water across Nafion. The increasing water flux at any flow rate with temperature seen in Fig. 6 shows that the temperature effect on the increase in the diffusion coefficient is more significant than the decrease in the water content gradient. The temperature correction to the diffusion coefficient is through the enthalpy term in Eq. 15. The enthalpy of diffusion was measured by Yeo and Eisenberg[22] for Nafion membranes were equilibrated with pure liquid water. The results of this work suggest that the enthalpy of diffusion is not affected by the introduction of HCl into the equilibrating solution.

Finally, to estimate the number of water molecules transported across the membrane from the anode to cathode, water flux measurements were made as a function of current density at 80 and 60°C. The flow rate of HCl was fixed at the 4500 cm^3/min (STP) and the applied current density varied from 0 to 1.0 A/cm^2 (0.8 A/cm^2 for the 60°C data). At such high flow rates of HCl, it is assumed that the current distribution and therefore the net flux of water is uniform across the membrane. A plot of the measured water flux *vs.* the applied current density is shown in Fig. 8. As can be seen from the figure, the flux of water decreased linearly with an increase in the applied current density. The number of moles of water transported with a mole of protons can be calculated from the slope of the straight line. The straight-line fits describing the data in the figure were obtained and the electro-osmotic drag parameter calculated. At 80 and 60°C, the electro-osmotic drag parameter was equal to 3.84 and 3.50, respectively. Zawodzinski *et al.*[12] measured a value of 2.5 for the electro-osmotic drag parameter when Nafion membranes were equilibrated with liquid water. Also, Balko *et al.*[21] measured a value of 2.5 for membranes equilibrated in 2.5 M hydrochloric acid solutions. A lower value in the range of 1.0-1.5 was measured for Nafion membranes equilibrated with water vapor.[15,17] The value we measured in this work is closer to the liquid water measurements by other researchers.[12,21]

Conclusions

In the presence of HCl, accurate predictions of the water flux across Nafion membranes are possible only with the inclusion of a condensed phase in the calculations. Due to the lowered equilibrium mole fraction of water vapor combined with a Fickian diffusion coefficient that is approximately a factor of five greater than the pure water case, water condenses even at high flow rates (<8000 cm^3/min). At high flow rates, the concentration of the condensed acid phase is uniform throughout and results in an asymptote in the water flux. The electro-osmotic drag parameter was fairly insensitive to temperature and was equal to 3.9 mol of water/mole of protons, at 80°C.

University of South Carolina assisted in meeting the publication costs of this article.

List of Symbols

a_w	activity of water
A	area of the flow channel, cm^2
C_{HCl}	concentration of HCl, mol/cm^3
C^e_{HCl}	equilibrium concentration of HCl in condensed phase, mol/cm^3
C^s_{HCl}	surface concentration of HCl in condensed phase, mol/cm^3
$\langle C_{HCl} \rangle$	average concentration of HCl in the condensed phase, mol/cm^3
d	depth of the flow channel, cm
D_{HCl}	diffusion coefficient of HCl, cm^2/s
$D_{w,F}$	Fickian diffusion coefficient of water, cm^2/s
$D_{w,I}$	self diffusion coefficient of water, cm^2/s
K	permeability of gas diffusion backing, cm^2
L	length of the flow channel, cm
L_c	condensation length, cm
L_{GDB}	length of gas diffusion backing, cm
M_M	molecular weight of membrane, cm
$N_{w,z}$	flux of water in the flow channel, mol/cm^2s
$N_{w,x}$	flux of water across the membrane, mol/cm^2s
N^o_{HCl}	inlet molar flow rate of HCl gas, mol/s
P	pressure, atm
P^*	vapor pressure of water, atm
Q^o_{HCl}	inlet volumetric flow rate of HCl gas, cm^3/s
Q^L	volumetric flow rate of condensed phase, cm^3/s
R	universal gas constant
T	temperature, K
V^L	velocity of condensed phase, cm/s
w_1	width of the flow channel, cm
w_2	width of the membrane, cm
x	distance perpendicular to membrane, cm
x^e_w	equilibrium mole fraction of water in liquid phase
y	distance perpendicular to the condensed phase, cm
y_w	mole fraction of water vapor in the flow channel
y^e_w	equilibrium mole fraction of water in vapor phase
z	distance along flow channel, cm

Greek

δ_M	thickness of the catalyst-coated membrane, cm
δ_z	thickness of the condensed phase, cm
δ^0	thickness of the condensed phase at $z = L$, cm
ΔP	pressure drop across the flow channel, dyn/cm^2
λ_a	water content of the membrane on the anode side
λ_c	water content of the membrane on the cathode side
λ^o	water content of the membrane when equilibrated with pure water
μ_{HCl}	viscosity of HCl solution, poise
ρ_{HCl}	density of HCl solution, g/cm^3
ρ_M	density of Nafion, g/cm^3

References

1. G. Pillay and C. Chen, *J. Electrochem. Soc.*, **143**, 3410 (1996).
2. F. Hine, *Electrode Processes and Electrochemical Engineering*, p. 127, Plenum Press, New York (1985).
3. F. Wattimena and W. M. H. Sachtler, *Stud. Surf. Sci. Catal.*, **7**, 816 (1981).
4. W. C. Schreiner, A. E. Cover, W. D. Hunter, C. P. Van Dijk, and H. S. Jongenburger, *Hydrolog. Process.*, **53**, 151 (1974).
5. T. Yasuaki, *Stud. Surf. Sci. Catal.*, **92**, 41 (1995).
6. J. A. Trainham, C. G. Law, J. S. Newman, K. B. Keating, and D. J. Eames, U.S. Pat. 5.411,641 (1995).
7. F. R. Minz, in *HCl-Electrolysis, Technology for Recycling Chlorine*, Bayer AG, Conference on Electrochemical Processing, Innovation, and Progress, Glasgow, Scotland (1993).
8. D. T. Mah, Abstract 948, p. 1186, The Electrochemical Society Meeting Abstracts, Vol. 96-1, Los Angeles, CA, May 5-10, 1996.
9. J. Trainham and F. Freire, Paper 10c, presented at 5th World Congress of Chemical Engineering, San Diego, CA, June 1996.
10. D. J. Eames and J. S. Newman, *J. Electrochem. Soc.*, **142**, 3619 (1995).
11. L. Burton, in *10th International Forum Electrolysis Chemical Industry, and Electrosynthesis*, p. 1, Lancaster, NY (1996).
12. T. A. Zawodzinski, T. E. Springer, J. Davey, R. Jestel, C. Lopez, J. Valerio, and S. Gottesfeld, *J. Electrochem. Soc.*, **140**, 1981 (1993).
13. T. A. Zawodzinski, M. Neeman, L. O. Sillerud, and S. Gottesfeld, *J. Phys. Chem.*, **95**, 6040 (1991).
14. T. A. Zawodzinski, T. E. Springer, F. Uribe, and S. Gottesfeld, *Solid State Ionics*, **60**, 199 (1993).
15. T. E. Springer, T. A. Zawodzinski, and S. Gottesfeld, *J. Electrochem. Soc.*, **138**, 2334 (1991).
16. T. A. Zawodzinski, C. Derouin, S. Radzinski, R. J. Sherman, V. T. Smith, T. E. Springer, and S. Gottesfeld, *J. Electrochem. Soc.*, **140**, 1041 (1993).
17. T. F. Fuller, Ph.D. Thesis, University of California, Berkeley (1992).
18. S. Motupally, A. J. Becker, and J. W. Weidner, *J. Electrochem. Soc.*, **147**, 3171 (2000).
19. *Environmental Simulation Program*, OLI Systems Inc., Murray Plains, NJ, USA.
20. D. M. Bernardi and M. Verbrugge, *AIChE J.*, **37**, 1151 (1990).
21. E. N. Balko, J. F. McElroy, and A. B. LaConti, *Int. J. Hydrogen Energy*, **6**, 577 (1987).
22. S. W. Yeo and A. Eisenberg, *J. Appl. Polym. Sci.*, **21**, 875 (1977).
23. R. A. Robinson and R. H. Stokes, *Electrolyte Solutions*, Butterworths, London (1961).
24. R. H. Perry and D. W. Green, *Perry's Chemical Engineering Handbook*, McGraw-Hill Professional Book Group, New York (1999).